

Quantum dissipation at conical intersections of quasienergies

Sigmund Kohler

Instituto de Ciencia de Materiales de Madrid, CSIC, E-28049 Madrid, Spain

(Dated: September 2, 2024)

We investigate the properties of Floquet states in the vicinity of a conical intersection of quasienergies and work out the consequences of the underlying spatio-temporal symmetries for a driven two-level system coupled to an ohmic heat bath. We find that on manifolds with constant quasienergy splitting, the mean energies of the Floquet states are continuously interchanged. In the presence of dissipation, the parameter dependence of the stationary populations generally resembles that of the mean energies. In turn, the mean energies are an indicator for the qualitative behavior of the density operator in the long-time limit. A further consequence of the symmetries is that for specific driving parameters, the stationary state may be fully mixed even at arbitrarily low temperatures. For large driving frequencies, such states with maximal entropy are found in the whole vicinity of the intersection, which can be explained by a chirality emerging in this limit. Analytical results beyond a high-frequency approximation are illustrated by numerical data.

I. INTRODUCTION

Floquet engineering is the construction of effective Hamiltonians by acting with ac fields or periodic pulses upon a quantum system. The idea originates in the suppression of tunneling in bistable systems [1] and tight-binding models [2]. It has been proposed also for many-particle states in double quantum dots [3], cold atoms [4, 5], and photonics [6]. Experimental realizations have been achieved with quantum dots [7–9], superconducting qubits [10, 11], and optical lattices [12]. These ideas have been extended to tuning topological properties [13, 14] and to artificial gauge fields [5, 15].

A theoretical tool for studying ac-driven systems is Floquet theory with its quasienergies [16, 17] which emerge in the formal expression for the propagator and, thus, provide much insight. For example, suppression of tunneling can be attributed to exact quasienergy crossings [1, 2] which require a spatio-temporal symmetry known as generalized parity [18, 19]. When a small perturbation such as a static detuning breaks this symmetry, the exact quasienergy crossings become avoided. Then, as will be shown, the quasienergy surfaces as a function of any original parameter and the detuning form a double cone with a degeneracy at the tip, a so-called conical or diabolical intersection. Conical intersections have been investigated mainly in the rather different context of breakdown of adiabaticity in Born-Oppenheimer theory, where both coherent [20–22] and dissipative [23, 24] time-evolution have been considered.

Dissipative transitions between Floquet states lack detailed balance [25]. Therefore, the stationary state generally is not a canonical ensemble, but must be computed with a quantum master equation [26, 27]. Even for minimal dissipation, the populations may significantly depend on the operator that couples the system to the environment [28–30]. Only in the high-frequency limit, one may find Floquet-Gibbs states, which are canonical states with eigenenergies replaced by quasienergies [31, 32]. In some cases, by contrast, the mean energies seem more relevant for the populations [33, 34]. For many of these

results, level crossings play an important role [9, 28–30, 33, 35]. In particular, it has been found [30] that in the absence of a static detuning, at exact quasienergy crossings, the populations of Floquet states may be discontinuous.

Here, we extend previous work [30] on the driven two-level system by considering the full conical intersection, i.e., by investigating the impact of an additional detuning. It will turn out that sufficiently close to the cone tip, the physics is widely determined by the symmetry operation responsible for the emergence of the crossing. Moreover, the analysis sheds light on the role of the mean energies for dissipative transitions between Floquet states.

In Sec. II we derive generic properties of the Floquet states in that region without resorting to a high-frequency limit. Section III is devoted to quantum dissipation, in particular to the populations of the Floquet states in the long-time limit, while conclusions are drawn in Sec. IV.

II. FLOQUET STATES AT CONICAL INTERSECTIONS

As a model, we consider the ac-driven two-level Hamiltonian

$$H(t) = \frac{\Delta}{2}\sigma_x + \frac{1}{2}[\varepsilon + A\cos(\Omega t)]\sigma_z, \quad (1)$$

with tunneling Δ , static detuning ε , driving amplitude A and frequency Ω , while σ_x and σ_z denote Pauli matrices.

Owing to time periodicity, the corresponding Schrödinger equation possesses a complete set of solutions of the form $e^{-iqt}|\phi(t)\rangle$ with quasienergy q and Floquet state $|\phi(t)\rangle$ which shares the time periodicity of the driving [16, 17]. Floquet states are eigensolutions of the operator $\mathcal{H} = H(t) - i\partial_t$ (in units with $\hbar = 1$). Quasienergies come in a Brillouin zone structure, i.e., for any $|\phi(t)\rangle$ and integer n , $|\phi^{(n)}(t)\rangle = e^{-in\Omega t}|\phi(t)\rangle$ is a physically equivalent Floquet state with quasienergy $q + n\Omega$. To characterize a Floquet state, one may employ

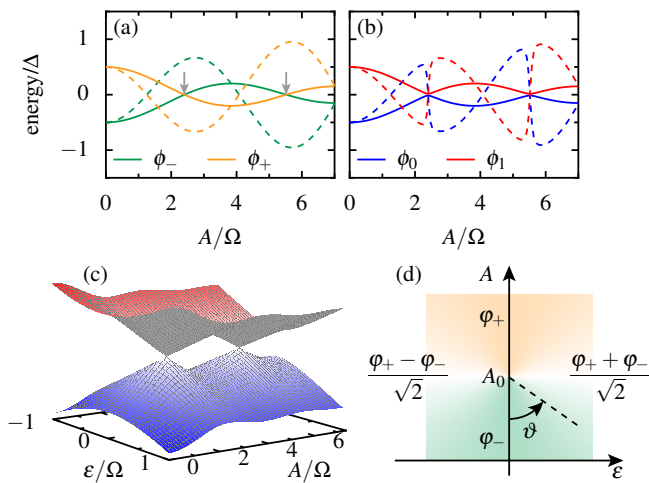


FIG. 1. (a) Quasienergies q_{\pm} (solid lines) and mean energies E_{\pm} (dashed) for driving frequency $\Omega = 25\Delta$ in the absence of a static detuning, such that the Floquet states possess definite generalized parity indicated by colors (green: even, orange: odd). We focus on the vicinity of the quasienergy crossings marked by grey arrows. (b) The same for static detuning $\varepsilon = 0.03\Delta$, i.e., in the absence of generalized parity. The color code now refers to the sign of the quasienergy. (c) Quasienergies q_0 and q_1 as a function of the detuning ε and the driving amplitude A . (d) Floquet state with lower quasienergy, $|\phi_0\rangle$, in the vicinity of a degeneracy point $(\varepsilon, A) = (0, A_0)$ in terms of the basis states $|\varphi_{\pm}\rangle$. The underlying color indicates the corresponding mean energy $E_0 = E_- \cos \vartheta$ [green: $E_0 > 0$, cf. panel (a)].

its mean energy E which is the expectation value of $H(t)$ averaged over the driving period. Equivalent states possess equal mean energy, as is expected for an observable. For the present purpose, it is convenient to consider Floquet states as elements of Sambe space which is the direct product of the underlying Hilbert space and the space of $2\pi/\Omega$ -periodic functions [17]. We denote its elements by a double angle, $|\phi\rangle\rangle$, where $|\phi(t)\rangle = \langle t|\phi\rangle\rangle$ and $E = q + \langle\langle\phi|i\partial_t|\phi\rangle\rangle$.

Hamiltonian (1) is invariant under time-reversal $t \rightarrow -t$ which allows one to write the Floquet state $|\phi(t)\rangle$ as Fourier series with real coefficients. Moreover, the chirality $C = i\sigma_y K$ with K denoting complex conjugation maps $\mathcal{H} \rightarrow -\mathcal{H}$, which implies that non-zero quasienergies come in pairs with opposite sign. Without loss of generality, we will choose the Floquet states from the Brillouin zone symmetric around zero, $-\Omega/2 \leq q < \Omega/2$, and label them such that $q_0 \leq 0$, $q_1 = -q_0$. Notice, however, that this order is arbitrary and by itself cannot justify designations such as “ground state”.

A \mathbb{Z}_2 symmetry with direct consequences for the physics discussed herein is the generalized parity $G = \sigma_x \exp(\pi\partial_t/\Omega)$ which consists of a unitary transformation with σ_x in Hilbert space and a time shift by half a period. It is present for $\varepsilon = 0$. Then, the Floquet states can be classified as even or odd depending on the respective eigenvalue ± 1 of G [18, 19]. Quasienergies of states with

different generalized parity may form exact crossings with accidental degeneracies. Also the mean energies may exhibit exact crossings which, however, need not coincide with the quasienergy crossings, see Fig. 1(a). Two properties of the generalized parity will turn out important. First, σ_x and $i\partial_t$ are even under transformation with G , while σ_z is odd. Second, from the above definition of the equivalent states in the time domain, it is obvious that for a Floquet state with generalized parity ± 1 , the equivalent state $|\phi^{(n)}\rangle\rangle$ has generalized parity $\pm(-1)^n$.

The situation changes in the presence of a detuning $\varepsilon \neq 0$. Then the Floquet states no longer possess generalized parity, and exact quasienergy crossings turn into avoided crossings, as can be witnessed in Fig. 1(b). This implies that the quasienergies are degenerate only at isolated points of parameter space (ε, A) . Therefore, they form accidental symmetry-allowed conical intersections, as is shown in Fig. 1(c). Henceforth, we focus on the vicinities of such intersections.

We employ degenerate perturbation theory using the Floquet states $|\varphi_{\pm}\rangle\rangle = \pm G|\phi_{\pm}\rangle\rangle$ for $H_0(t) \equiv \frac{1}{2}\Delta\sigma_x + \frac{1}{2}A_0\sigma_z \cos(\Omega t)$ as zeroth order, where A_0 denotes the driving amplitude at the respective quasienergy crossing (the notation φ_{\pm} is restricted to $\varepsilon = 0$ and $A = A_0$). In the basis chosen, $i\partial_t = G^\dagger i\partial_t G$ and $\sigma_x = G^\dagger \sigma_x G$ are diagonal, while $\sigma_z = -G^\dagger \sigma_z G$ is off-diagonal. For large Ω , the amplitude at the crossing, A_0 , can be expressed with a root of a Bessel function [19], but the present investigation is not restricted to this limit. Let us emphasize that while the $|\varphi_{\pm}(t)\rangle\rangle$ form a basis of the Hilbert space, the full Sambe space is spanned by all $|\varphi_{\pm}^{(n)}\rangle\rangle$. By evaluating the matrix elements of $H_1(t) = H(t) - H_0(t)$ in the subspace considered, one finds the time-independent perturbation $H'_1 = \frac{1}{2}(a\sigma'_z + b\sigma'_x)$ with

$$a = \frac{A_0 - A}{A_0} (2E_- + \Delta \langle\langle\varphi_-|\sigma_x|\varphi_- \rangle\rangle) \equiv r \cos \vartheta, \quad (2)$$

$$b = \varepsilon \langle\langle\varphi_-|\sigma_z|\varphi_+ \rangle\rangle \equiv r \sin \vartheta, \quad (3)$$

where $r = \sqrt{a^2 + b^2}$ measures the distance to the cone tip. Hence, the perturbation theory holds for $r \ll \Omega, \varepsilon$. Unlike in the usual high-frequency approximation (see the Appendix), the present approach does not require $\Delta \ll \Omega$ as long as $|A - A_0| \ll A_0$. The prime refers to the time-dependent basis given by the states $|\varphi_{\pm}(t)\rangle\rangle$ with the mean energies $E_{\pm} = \langle\langle\varphi_{\pm}|H(t)|\varphi_{\pm}\rangle\rangle$. To obtain the expression for a , we have written the perturbation $(A - A_0)\sigma_z \cos(\Omega t)$ in terms of $H_0(t) - i\partial_t$ whose eigenvalues are the quasienergies q_{\pm} which for $A = A_0$ vanish according to the definition of A_0 . Moreover, we have used the already mentioned relation $E_{\pm} = q_{\pm} + \langle\langle\varphi_{\pm}|i\partial_t|\varphi_{\pm}\rangle\rangle$.

Diagonalization of H'_1 provides the perturbed Floquet states

$$|\phi_0\rangle\rangle = \cos(\vartheta/2)|\varphi_-\rangle\rangle + \sin(\vartheta/2)|\varphi_+\rangle\rangle \quad (4)$$

$$|\phi_1\rangle\rangle = -\sin(\vartheta/2)|\varphi_-\rangle\rangle + \cos(\vartheta/2)|\varphi_+\rangle\rangle \quad (5)$$

and their quasienergies $q_{0,1} = \pm r/2$. Since the off-diagonal matrix element $\langle\langle\varphi_+|i\partial_t|\varphi_-\rangle\rangle = 0$, the corre-

sponding mean energies read

$$E_0 = E_- \cos \vartheta = -E_1. \quad (6)$$

Figure 1(d) visualizes the definition of the angle ϑ and the result of the perturbation theory. Interestingly, values of ϑ that differ by π give rise to the following duality. Upon the shift $\vartheta \rightarrow \vartheta + \pi$, $|\phi_0(t)\rangle$ becomes proportional to $|\phi_1(t)\rangle$ and vice versa. However, while the shape of the Floquet states is interchanged, their quasienergies remain the same, i.e., $q_0 < 0$ and $q_1 > 1$ for all values of ϑ .

A central ingredient of our analysis will be the action of the generalized parity operator G on the Floquet states and their equivalent states. Using $G|\varphi_{\pm}^{(n)}\rangle = \pm(-1)^n|\varphi_{\pm}^{(n)}\rangle$, one obtains from Eqs. (4) and (5) the relations

$$G|\phi_0^{(n)}\rangle = (-1)^n \left(-|\phi_0^{(n)}\rangle \cos \vartheta + |\phi_1^{(n)}\rangle \sin \vartheta \right), \quad (7)$$

$$G|\phi_1^{(n)}\rangle = (-1)^n \left(|\phi_0^{(n)}\rangle \sin \vartheta + |\phi_1^{(n)}\rangle \cos \vartheta \right). \quad (8)$$

For the particular value $\vartheta = \pm\pi/2$, G maps the one Floquet state to the other, i.e. $G|\phi_0^{(n)}\rangle \propto |\phi_1^{(n)}\rangle$ and $G|\phi_1^{(n)}\rangle \propto |\phi_0^{(n)}\rangle$. Henceforth, we use the relations derived in this section to draw conclusions on the stationary state established by the coupling to a heat bath.

III. DISSIPATION AND STATIONARY STATE

To describe quantum dissipation, we couple the driven system to a heat bath modeled as harmonic oscillators with the Hamiltonians [36–39] $H_{\text{bath}} = \sum_{\nu} \omega_{\nu} a_{\nu}^{\dagger} a_{\nu}$ and $H_{\text{int}} = S\xi$, where $\xi = \sum_{\nu} \lambda_{\nu} (a_{\nu}^{\dagger} + a_{\nu})$ is a collective bath coordinate and S a system coordinate to be specified later. The influence of the bath is determined by its spectral density $J(\omega) = \pi \sum_{\nu} \lambda_{\nu}^2 \delta(\omega - \omega_{\nu})$ and the correlation function $C(t) = \langle \xi(0)\xi(t) \rangle$. At thermal equilibrium, the latter in frequency space reads $C(\omega) = 2J(\omega)n_{\text{th}}(\omega)$ with the bosonic occupation number $n_{\text{th}}(\omega) = [\exp(\omega/k_B T) - 1]^{-1}$ and temperature T . All numerical results presented below are computed with an ohmic spectral density $J(\omega) = \pi\alpha\omega/2$ with dimensionless coupling strength α [36]. For the analytical arguments, however, it will only be relevant that $J(\omega)$ smoothly vanishes for $\omega \rightarrow 0$.

Focussing on weak dissipation, we employ the Floquet-Bloch-Redfield formalism of Refs. [27, 29] which provides a master equation in Floquet basis of the form $\dot{\rho}_{\alpha\alpha'}(t) = \sum_{\beta,\beta'} \mathcal{L}_{\alpha\alpha',\beta\beta'}(t)\rho_{\beta\beta'}(t)$. Generally, the Liouvillian \mathcal{L} is $2\pi/\Omega$ -periodic, but within a rotating-wave approximation can be replaced by its time-average. While this formulation is suitable for computational purposes, for our analytical treatment we employ a secular approximation. For $\alpha \ll 1$ the density operator eventually becomes diagonal [27], such that the stationary state can be computed from the Pauli-type master equation

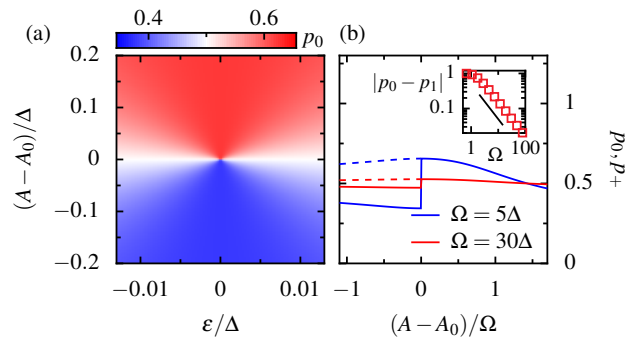


FIG. 2. (a) Population p_0 of the Floquet state with lower quasienergy as a function of the detuning ε and the distance of the amplitude to the crossing, $A - A_0$, where $A_0 \approx 2.4\Omega$ is the smallest driving amplitude at which the quasienergies cross for $\Omega = 5\Delta$. The bath with temperature $T = 0.01\Delta/k_B$ is coupled with strength $\alpha = 0.01$ via $S = \sigma_x$. (b) Population p_0 (solid line) for $\varepsilon = 0$ exhibiting a discontinuity at $A = A_0$ visible as step. The dashed line depicts the population of the Floquet state with even generalized parity, $|\phi_+\rangle$, which is continuous. Inset: Discontinuity of p_0 at the intersection as a function of the driving frequency Ω . The solid line indicates a decay $\propto 1/\Omega$.

$\dot{p}_\alpha = \sum_{\beta} (\Gamma_{\alpha\beta} p_\beta - \Gamma_{\beta\alpha} p_\alpha)$ for the Floquet-state populations p_α with the golden-rule rates [26, 27, 40]

$$\Gamma_{\alpha\beta} = \sum_k C(q_\alpha - q_\beta + k\Omega) |S_{\alpha\beta,k}|^2, \quad (9)$$

where $S_{\alpha\beta,k}$ denotes the k th Fourier component of the time-dependent transition matrix element $S_{\alpha\beta}(t) = \langle \phi_\alpha(t) | S | \phi_\beta(t) \rangle$. In Sambe formalism, it can be written as $S_{\alpha\beta,k} = \langle \langle \phi_\alpha | S | \phi_\beta^{(k)} \rangle \rangle = \langle \langle \phi_\beta | S | \phi_\alpha^{(-k)} \rangle \rangle^*$, which allows an elegant formulation of the symmetry properties.

Close to an intersection, the correlation function $C(\omega)$ in Eq. (9) is evaluated at the frequencies $\omega = \pm r + k\Omega$, where the quasienergy splitting obeys $r \ll \Omega$. Therefore, r can generally be neglected, such that the dissipative rates depend only on the basis states $|\varphi_{\pm}\rangle$ and the angle ϑ . However, there exist also exceptional cases in which $S_{\alpha\beta}(t)$ is practically time-independent, such that in Eq. (9) the term with $k = 0$ dominates. Then $\Gamma_{\alpha\beta}$ is formally given by the corresponding expression for a time-independent problem, but with the eigenenergies replaced by quasienergies, which is the constituting feature of a Floquet-Gibbs state [31, 32].

A. The generic behavior

We start with a bath coupling via $S = \sigma_x$ which represents the generic case in which the Fourier coefficients $S_{\alpha\beta,k}$ with $k \neq 0$ dominate, such that r can be neglected. As already discussed, upon $\vartheta \rightarrow \vartheta + \pi$ the Floquet states (4) and (5) are interchanged. Consequently, the transition rates Γ_{01} and Γ_{10} and, thus, the populations p_0 and

p_1 are interchanged as well, i.e., p_0 at an angle ϑ must be equal to $p_1 = 1 - p_0$ at $\vartheta + \pi$. In short, the stationary populations exhibit the duality of the Floquet states, such that $p_0 - 1/2$ turns out anti-symmetric upon point reflection at the cone tip $(0, A_0)$, which is confirmed by the numerical data shown in Fig. 2(a). The same reasoning can be applied to the mean energy with the conclusion that E_0 must change from E_- for $\vartheta = 0$ to E_+ for $\vartheta = \pi$ in agreement with the result of the perturbation theory in Eq. (6). Therefore the population difference $p_0 - p_1$ and the mean energy difference $E_1 - E_0$ vary in the same way. Interestingly, this includes a sign change of $p_0 - p_1$ on a manifold with constant quasienergy splitting. On a line through the tip, this leads to discontinuity which can be attributed to the discontinuities of the Floquet states (4) and (5) [30]. In a continuous basis such as the one formed by the states with definite generalized parity along the A -axis, by contrast, the populations are continuous as well. This is verified by the dashed lines in Fig. 2(b).

Since the populations as a function of ϑ change from $p_0 < p_1$ to the opposite order, there exists some values for which $p_0 = p_1 = 1/2$, provided that the behavior is continuous. Figure 2(a) suggests, that this occurs at $\vartheta = \pm\pi/2$. For a proof, we use $G^\dagger \sigma_x G = \sigma_x$ together with Eqs. (7) and (8). For $\vartheta = \pm\pi/2$ this provides the relation $S_{01,k} = \langle\langle \phi_0 | G^\dagger \sigma_x G | \phi_1^{(k)} \rangle\rangle = (-1)^k S_{10,k}$. Therefore, all terms that contribute to the transition rate Γ_{01} also occur in the expression for Γ_{10} such that $\Gamma_{01} = \Gamma_{10}$ and, thus, $p_0 = p_1$. In other words, the stationary density operator is proportional to the unit matrix, i.e., it describes a fully incoherent mixture irrespective of the temperature. Such equal population of both Floquet states is particularly interesting, because it can be detected by dispersive readout, i.e., it leaves its fingerprints in the transmission of a cavity coupled to the two-level system, as has been demonstrated in a recent experiment [9].

The symmetry properties discussed so far hold for any driving frequency $\Omega \gtrsim \Delta$. Within the usual high-frequency approximation [19] (for a summary, see the Appendix), we find a further symmetry relation. It is based on the transformation with σ_z , which in the Hamiltonian (1) inverts the sign of the tunnel term, effectively causing $\Delta \rightarrow -\Delta$. Since for large frequencies the quasienergies read $q_{0,1} = \mp(\Delta/2)J_0(A/\Omega)$ [19], the state $\sigma_z|\phi_0(t)\rangle$ must be proportional to the Floquet state with opposite quasienergy, i.e., $\sigma_z|\phi_0(t)\rangle \propto |\phi_1(t)\rangle$ and vice versa. Thus, for any value of ϑ , σ_z acts on the Floquet states like the generalized parity operator G for the particular value $\vartheta = \pi/2$. Therefore, we expect to find in the high-frequency limit the same consequences, but now in the whole vicinity of the intersection. Specifically, for any ϑ , the stationary state is fully mixed state with $p_0 = p_1 = 1/2$.

It is interesting to see how finite-frequency corrections vanish with increasing Ω . The inset of Fig. 2(b) reveals that the limit is approached $\propto 1/\Omega$. Even for $\Omega = 15\Delta$, the difference ~ 0.1 is still remarkably large.

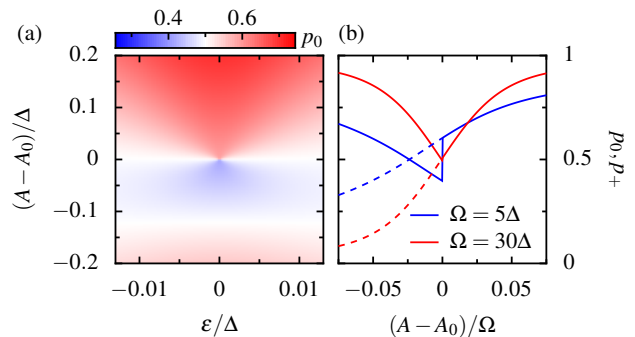


FIG. 3. The same as Fig. 2 but for a bath coupling via $S = \sigma_z$.

Thus, while the usual high-frequency approximation for the quasienergies is reliable for $\Omega \gtrsim 2\Delta$ [19], we observe that the approximation describes dissipative effects well only for larger frequencies.

B. Coupling via σ_z and Floquet-Gibbs state

A bath coupling via $S = \sigma_z$ anti-commutes with the generalized parity operator and, thus, $G^\dagger \sigma_z G = -\sigma_z$. Then the symmetry relation for the matrix element of S acquires a minus sign such that $S_{01,k} = (-1)^{k+1} S_{10,k}$. Since the rates $\Gamma_{\alpha\beta}$ depend only on absolute values, the generic behavior discussed above should be found as well. However, as we can appreciate in Fig. 3(a), this is the case only very close to the intersection, while for a slightly smaller amplitude, the population of ϕ_0 becomes much larger. The reason for this is that there the Fourier component with $k = 0$ dominates. This becomes clear when computing the matrix elements within the usual high-frequency approximation, $\langle \phi_0(t) | \sigma_z | \phi_1(t) \rangle = -1$, which can be easily verified by the explicit expressions given in the Appendix. Hence, $S_{10}(t)$ is time independent such that $S_{\alpha\beta,k}$ vanishes unless $k = 0$. Therefore, as discussed above, we expect to find a Floquet-Gibbs state. Indeed the conditions for the emergence of such state formulated in Refs. [31, 32] are fulfilled, namely the driving frequency is very large, while the driving and the system-bath coupling commute at all times.

We are also interested in intermediate frequencies for which components with $k \neq 0$ still contribute. Very close to the intersection, r is sufficiently small such that the term with $k = 0$ may be neglected. Then the population p_0 still resembles the generic case, including the discontinuity at A_0 . When moving away from the intersection, however, r grows such that the contribution of $S_{\alpha\beta,0}$ becomes increasingly important and one observes a crossover from the generic behavior to a Floquet-Gibbs state. Data along the A -axis in Fig. 3(b) verify that for $\Omega = 5\Delta$, features of the generic behavior are still present. With increasing frequency, the crossover region shrinks and eventually disappears.

As mentioned above, equal Floquet state population

can be detected by coupling the driven system to a cavity [9]. Therefore, the crossover to a Floquet-Gibbs state may be tested experimentally as well. Such measurement may provide evidence for a system-bath coupling via σ_z .

C. Mixed bath coupling

One might suppose that at least for moderate driving frequency, a bath coupling via any linear combination of Pauli matrices $S = \sum_i c_i \sigma_i$ would also lead to the generic behavior depicted in Fig. 2(a). Now, by contrast, the condition of S being either even or odd under generalized parity no longer holds. Since σ_x is even while σ_y and σ_z are odd, the requirement is met only if either $c_1 = 0$ or $c_2 = c_3 = 0$. For a visualization of the crossover, we consider a bath coupling via

$$S = \sigma_x \sin \theta + \sigma_z \cos \theta. \quad (10)$$

Figure 4 shows the population p_0 for various values of the coupling angle θ . In consistency with Refs. [29, 30], it shows that the coupling via σ_z is rather sensitive to any small admixture of σ_x . Already for a rather small value of θ , the Floquet-Gibbs state is lost. With increasing mixing angle θ , the line with equal population $p_0 = p_1 = 1/2$ turns smoothly into the one for pure σ_x coupling.

D. Global picture

While we have worked out the scenario in the vicinities of conical intersections, it remains to integrate these findings into a global picture. Therefore, we show in Fig. 5 the population in a much larger parameter range. The stripes with equal population (white) indicate that the choice of S influences the global behavior significantly. For a coupling via σ_x , they are merely bent, but nevertheless extend over a rather large range. For σ_z , by contrast, the switching between the generic behavior and the Floquet-Gibbs state brings about a further line with $p_0 = 1/2$.

IV. CONCLUSIONS

We have worked out features of the driven two-level system in the vicinity of conical intersections of quasienergies, which can be derived from the behavior under transformation with the generalized parity operator. In the absence of a detuning, the according symmetry is responsible for the emergence of exact crossings. For a small detuning, i.e., when the Hamiltonian no longer obeys generalized parity, we found various generic properties of the Floquet states, foremost, the behavior of the mean energies and of the dissipative transition rates. The analytical achievements are based on a rotating-wave approximation which, as our numerical results verify, holds even for relatively small driving frequencies of

the order of the tunnel matrix element. In particular, we did not employ the common high-frequency approximation with Bessel functions.

While the quasienergies form a double cone, the mean energies exhibit a more intricate structure. On manifolds with constant quasienergies, they are continuously interchanged. Generally, the same happens for the populations of the Floquet states in the stationary limit. Therefore, the mean energies rather than the quasienergies provide an indication for the populations. Moreover, the sign change of the population difference implies the existence of fully mixed stationary states characterized by equal population of both Floquet states. In the high-frequency limit, such maximal entropy states are found in the whole vicinity of the intersection, which follows from a hidden chirality. An exceptional case is realized when the system-bath coupling commutes with the driving. Then the generic behavior of the populations, including the discontinuity along the amplitude axis, is found only for intermediate driving frequencies in a limited region. With increasing frequency, this region shrinks and eventually a Floquet-Gibbs state is formed.

At a larger distance from the cone, we find that the shape of the manifolds with maximal entropy depends on the system-bath interaction operator. By coupling in addition the two-level system to a microwave cavity, one can in principle find experimental signatures for equal Floquet state population [9]. Such measurements may provide evidence for the crossover from the generic behavior governed by mean energies to a Floquet-Gibbs state and, hence, for the type of bath coupling.

ACKNOWLEDGMENTS

This work was supported by the Spanish Ministry of Science, Innovation, and Universities (Grant No. PID2020-117787GB-I00), and by the CSIC Research Platform on Quantum Technologies PTI-001.

Appendix A: High-frequency approximation

For completeness and reference, we provide the known expressions for the Floquet states in the limit of large driving frequencies [19],

$$|\phi_{\pm}(t)\rangle = \frac{1}{\sqrt{2}} \begin{pmatrix} \pm e^{-iF(t)} \\ e^{iF(t)} \end{pmatrix}, \quad (A1)$$

with $F(t) = (A/2\Omega) \sin(\Omega t)$ and their quasienergies

$$q_{\pm} = \pm \frac{\Delta}{2} J_0(A/\Omega) \quad (A2)$$

with J_0 the zeroth-order Bessel function of the first kind. Thus, the position A_0 of any conical intersection requires that A_0/Ω matches a root of J_0 .

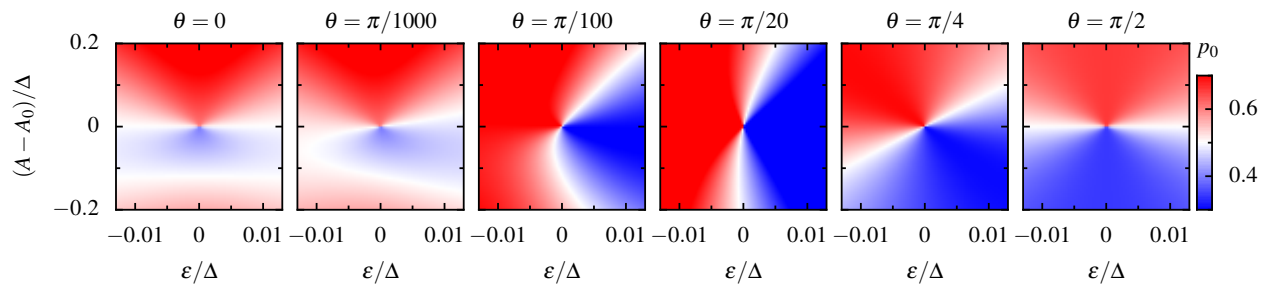


FIG. 4. Population of the Floquet state ϕ_0 for system-bath coupling via the operator S defined in Eq. (10) with the angle θ given on the top of each panel. The driving frequency is $\Omega = 8\Delta$.

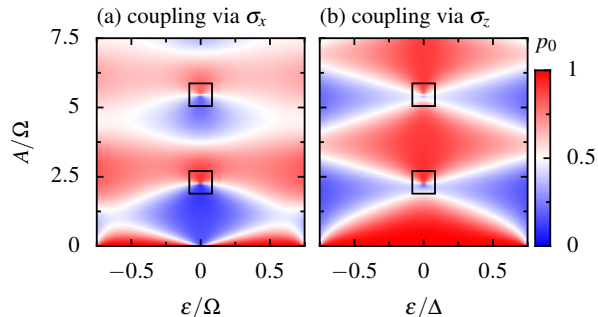


FIG. 5. Floquet state populations for bath coupling via σ_x (a) and σ_z (b), respectively, cf. Figs. 2(a) and 3(a). The driving frequency $\Omega = 1.5\Delta$ is chosen rather low, such that in panel (b) the zone with deviations from the Floquet-Gibbs state at $\varepsilon = 0$ and $A \lesssim A_0$ becomes visible. All other parameters are as in Fig. 2. The rectangles mark the conical intersections.

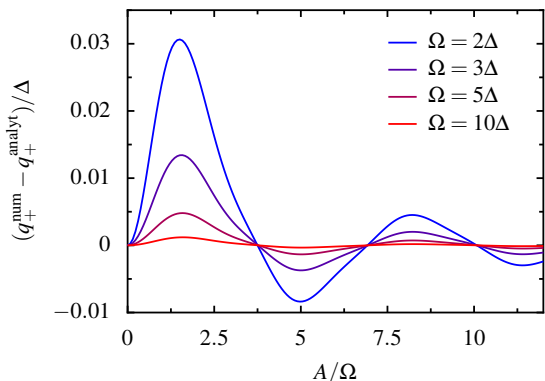


FIG. 6. Difference of the numerically computed quasienergy and the analytical approximation in Eq. (A2) as a function of the driving amplitude.

For a derivation of Eqs. (A1) and (A2) [19], one uses the Hamiltonian in the absence of the tun-

nel term as zeroth order, $H_0(t) = (A/2)\sigma_z \cos(\Omega t)$, where the corresponding propagator reads $U_0(t) = \exp[-i(A/2\Omega)\sigma_x \sin(\Omega t)]$. Transformation of the remaining contribution, $H_1 = (\Delta/2)\sigma_z$ with U_0 and subsequent time-average, i.e. a rotating-wave approximation, yields $H'_1 = (\Delta/2)J_0(A/\Omega)\sigma_x$. Its eigenvalues are the quasienergies (A2), while the Floquet states in Eq. (A1) are the eigenstates of H' transformed back to the Schrödinger picture. Figure 6 shows that already for $\Omega \gtrsim 2\Delta$, the approximation in Eq. (A2) deviates from the exact value by only a few percent of the tunnel matrix element Δ .

A particular feature of the Floquet states in Eq. (A1) is that the transition matrix element $\langle \phi_+(t) | \sigma_z | \phi_-(t) \rangle = -1$ is time-independent. For $\vartheta = 0$, we have $\phi_0 = \phi_-$ and $\phi_1 = \phi_+$ (and vice versa for $\vartheta = \pi$) such that only the Fourier component with $k = 0$ contributes to the dissipative rates Γ_{01} and Γ_{10} . For sufficiently large driving frequency, this finally leads to the emergence of a Floquet-Gibbs state [31, 32]. For intermediate Ω , however, components with $k \neq 0$ still play a role such that sufficiently close to A_0 , the generic behavior is restored.

Within high-frequency approximation, the Floquet states possess a further symmetry, namely a hidden chirality given by a transformation with σ_z . Obviously, in the Hamiltonian in Eq. (1) of the main text, the terms with the detunings ε and $A \cos(\Omega t)$ are invariant under transformation with σ_z . By contrast, the tunnel term changes sign, effectively causing $\Delta \rightarrow -\Delta$. Thus, already from Eq. (A2) it becomes clear that $\sigma_z |\phi_0(t)\rangle$ and $|\phi_1(t)\rangle$ can differ at most by a phase factor. For the choice of the phases of the Floquet states in Eq. (A1), one finds

$$\sigma_z |\phi_{\pm}(t)\rangle = -|\phi_{\mp}(t)\rangle. \quad (\text{A3})$$

Relations of this kind are typically found as consequence of a chirality, i.e., a mapping that inverts the sign of the Hamiltonian. Notice that σ_z and, thus, the relation $\sigma_z H'_1 \sigma_z = -H'_1$ are not affected by the back transformation to the Schrödinger picture.

[1] F. Grossmann, T. Dittrich, P. Jung, and P. Hänggi, Coherent destruction of tunneling, *Phys. Rev. Lett.* **67**, 516

(1991).

- [2] M. Holthaus, Collapse of minibands in far-infrared irradiated superlattices, *Phys. Rev. Lett.* **69**, 351 (1992).
- [3] C. E. Creffield and G. Platero, ac-driven localization in a two-electron quantum dot molecule, *Phys. Rev. B* **65**, 113304 (2002).
- [4] J. Gong, L. Morales-Molina, and P. Hänggi, Many-body coherent destruction of tunneling, *Phys. Rev. Lett.* **103**, 133002 (2009).
- [5] A. Eckardt, Colloquium: Atomic quantum gases in periodically driven optical lattices, *Rev. Mod. Phys.* **89**, 011004 (2017).
- [6] S. Longhi, Many-body coherent destruction of tunneling in photonic lattices, *Phys. Rev. A* **83**, 034102 (2011).
- [7] J. Stehlik, Y. Dovzhenko, J. R. Petta, J. R. Johansson, F. Nori, H. Lu, and A. C. Gossard, Landau-Zener-Stückelberg interferometry of a single electron charge qubit, *Phys. Rev. B* **86**, 121303(R) (2012).
- [8] F. Forster, G. Petersen, S. Manus, P. Hänggi, D. Schuh, W. Wegscheider, S. Kohler, and S. Ludwig, Characterization of qubit dephasing by Landau-Zener-Stückelberg-Majorana interferometry, *Phys. Rev. Lett.* **112**, 116803 (2014).
- [9] M.-B. Chen, B.-C. Wang, S. Kohler, Y. Kang, T. Lin, S.-S. Gu, H.-O. Li, G.-C. Guo, X. Hu, H.-W. Jiang, G. Cao, and G.-P. Guo, Floquet state depletion in ac-driven circuit QED, *Phys. Rev. B* **103**, 205428 (2021).
- [10] M. Sillanpää, T. Lehtinen, A. Paila, Y. Makhlin, and P. Hakonen, Continuous-time monitoring of Landau-Zener interference in a Cooper-pair box, *Phys. Rev. Lett.* **96**, 187002 (2006).
- [11] D. M. Berns, M. S. Rudner, S. O. Valenzuela, K. K. Berggren, W. D. Oliver, L. S. Levitov, and T. P. Orlando, Amplitude spectroscopy of a solid-state artificial atom, *Nature (London)* **455**, 51 (2008).
- [12] H. Lignier, C. Sias, D. Ciampini, Y. Singh, A. Zenesini, O. Morsch, and E. Arimondo, Dynamical control of matter-wave tunneling in periodic potentials, *Phys. Rev. Lett.* **99**, 220403 (2007).
- [13] A. Gómez-León and G. Platero, Floquet-Bloch theory and topology in periodically driven lattices, *Phys. Rev. Lett.* **110**, 200403 (2013).
- [14] M. Atala, M. Aidelsburger, J. T. Barreiro, D. Abanin, T. Kitagawa, E. Demler, and I. Bloch, Direct measurement of the Zak phase in topological Bloch bands, *Nat. Phys.* **9**, 795 (2013).
- [15] M. Aidelsburger, S. Nascimbène, and N. Goldman, Artificial gauge fields in materials and engineered systems, *C. R. Physique* **19**, 394 (2018).
- [16] J. H. Shirley, Solution of the Schrödinger equation with a Hamiltonian periodic in time, *Phys. Rev.* **138**, B979 (1965).
- [17] H. Sambe, Steady states and quasienergies of a quantum-mechanical system in an oscillating field, *Phys. Rev. A* **7**, 2203 (1973).
- [18] A. Peres, Dynamical quasidegeneracies and quantum tunneling, *Phys. Rev. Lett.* **67**, 158 (1991).
- [19] F. Großmann and P. Hänggi, Localization in a driven two-level dynamics, *Europhys. Lett.* **18**, 571 (1992).
- [20] D. R. Yarkony, Diabolical conical intersections, *Rev. Mod. Phys.* **68**, 985 (1996).
- [21] W. Domcke, D. R. Yarkony, and H. Köppel, eds., *Conical Intersections*, Advanced Series in Physical Chemistry, Vol. 17 (World Scientific, Singapore, 2011).
- [22] J. Larson, E. Sjöqvist, and P. Öhberg, *Conical Intersections in Physics: An Introduction to Synthetic Gauge Theories*, 1st ed., Lecture Notes in Physics, Vol. 965 (Springer, Heidelberg, 2020).
- [23] L. Chen, M. F. Gelin, V. Y. Chernyak, W. Domcke, and Y. Zhao, Dissipative dynamics at conical intersections: Simulations with the hierarchy equations of motion method, *Faraday Discuss.* **194**, 61 (2016).
- [24] H.-G. Duan and M. Thorwart, Quantum mechanical wave packet dynamics at a conical intersection with strong vibrational dissipation, *J. Phys. Chem. Lett.* **7**, 382 (2016).
- [25] S. Kohler, J. Lehmann, and P. Hänggi, Driven transport on the nanoscale, *Phys. Rep.* **406**, 379 (2005).
- [26] R. Blümel, A. Buchleitner, R. Graham, L. Sirko, U. Smilansky, and H. Walther, Dynamical localisation in the microwave interaction of Rydberg atoms: The influence of noise, *Phys. Rev. A* **44**, 4521 (1991).
- [27] S. Kohler, T. Dittrich, and P. Hänggi, Floquet-Markovian description of the parametrically driven, dissipative harmonic quantum oscillator, *Phys. Rev. E* **55**, 300 (1997).
- [28] A. Ferrón, D. Domínguez, and M. J. Sánchez, Tailoring population inversion in Landau-Zener-Stückelberg interferometry of flux qubits, *Phys. Rev. Lett.* **109**, 237005 (2012).
- [29] R. Blattmann, P. Hänggi, and S. Kohler, Qubit interference at avoided crossings: The role of driving shape and bath coupling, *Phys. Rev. A* **91**, 042109 (2015).
- [30] G. Engelhardt, G. Platero, and J. Cao, Discontinuities in driven spin-boson systems due to coherent destruction of tunneling: Breakdown of the Floquet-Gibbs distribution, *Phys. Rev. Lett.* **123**, 120602 (2019).
- [31] T. Shirai, T. Mori, and S. Miyashita, Condition for emergence of the Floquet-Gibbs state in periodically driven open systems, *Phys. Rev. E* **91**, 030101(R) (2015).
- [32] T. Shirai, J. Thingna, T. Mori, S. Denisov, P. Hänggi, and S. Miyashita, Effective Floquet-Gibbs states for dissipative quantum systems, *New J. Phys.* **18**, 053008 (2016).
- [33] S. Kohler, R. Utermann, P. Hänggi, and T. Dittrich, Coherent and incoherent chaotic tunneling near singlet-doublet crossings, *Phys. Rev. E* **58**, 7219 (1998).
- [34] R. Ketzmerick and W. Wustmann, Statistical mechanics of Floquet systems with regular and chaotic states, *Phys. Rev. E* **82**, 021114 (2010).
- [35] O. V. Ivakhnenko, S. N. Shevchenko, and F. Nori, Nonadiabatic Landau-Zener-Stückelberg-Majorana transitions, dynamics, and interference, *Phys. Rep.* **995**, 1 (2023).
- [36] A. J. Leggett, S. Chakravarty, A. T. Dorsey, M. P. A. Fisher, A. Garg, and W. Zwerger, Dynamics of the dissipative two-state system, *Rev. Mod. Phys.* **59**, 1 (1987).
- [37] P. Hänggi, P. Talkner, and M. Borkovec, Reaction-rate theory: Fifty years after Kramers, *Rev. Mod. Phys.* **62**, 251 (1990).
- [38] U. Weiss, *Quantum Dissipative Systems*, 4th ed. (World Scientific, Singapore, 2012).
- [39] G. T. Landi, D. Poletti, and G. Schaller, Nonequilibrium boundary-driven quantum systems: Models, methods, and properties, *Rev. Mod. Phys.* **94**, 045006 (2022).
- [40] M. Grifoni and P. Hänggi, Driven quantum tunneling, *Phys. Rep.* **304**, 229 (1998).